AJNR

Contrast Leakage Patterns from Dynamic Susceptibility Contrast Perfusion MRI in the Grading of Primary Pediatric Brain Tumors

C.Y. Ho, J.S. Cardinal, A.P. Kamer, C. Lin and S.F Kralik

AJNR Am J Neuroradiol 2016, 37 (3) 544-551
doi: https://doi.org/10.3174/ajnr.A4559
http://www.ajnr.org/content/37/3/544

Contrast Leakage Patterns from Dynamic Susceptibility Contrast Perfusion MRI in the Grading of Primary Pediatric Brain Tumors

C.Y. Ho, J.S. Cardinal, A.P. Kamer, C. Lin, and S.F Kralik

ABSTRACT

BACKGROUND AND PURPOSE: The pattern of contrast leakage from DSC tissue signal intensity time curves have shown utility in distinguishing adult brain neoplasms, but has limited description in the literature for pediatric brain tumors. The purpose of this study is to evaluate the utility of grading pediatric brain tumors with this technique.

MATERIALS AND METHODS: A retrospective review of tissue signal-intensity time curves from 63 pediatric brain tumors with preoperative DSC perfusion MR imaging was performed independently by 2 neuroradiologists. Tissue signal-intensity time curves were generated from ROIs placed in the highest perceived tumor relative CBV. The postbolus portion of the curve was independently classified as returning to baseline, continuing above baseline (T1-dominant contrast leakage), or failing to return to baseline (T2*-dominant contrast leakage). Interobserver agreement of curve classification was evaluated by using the Cohen κ. A consensus classification of curve type was obtained in discrepant cases, and the consensus classification was compared with tumor histology and World Health Organization grade.

RESULTS: Tissue signal-intensity time curve classification concordance was 0.69 (95% CI, 0.54–0.84) overall and 0.79 (95% CI, 0.59–0.91) for a T1-dominant contrast leakage pattern. Twenty-five of 25 tumors with consensus T1-dominant contrast leakage were low-grade (positive predictive value, 1.0; 95% CI, 0.83–1.00). By comparison, tumors with consensus T2*-dominant contrast leakage or return to baseline were predominantly high-grade (10/15 and 15/23, respectively) with a high negative predictive value (1.0; 95% CI, 0.83–1.0). For pilomyxoid or pilocytic astrocytomas, a T1-dominant leak demonstrated high sensitivity (0.91; 95% CI, 0.70–0.98) and specificity (0.90, 95% CI, 0.75–0.97).

CONCLUSIONS: There was good interobserver agreement in the classification of DSC perfusion tissue signal-intensity time curves for pediatric brain tumors, particularly for T1-dominant leakage. Among patients with pediatric brain tumors, a T1-dominant leakage pattern is highly specific for a low-grade tumor and demonstrates high sensitivity and specificity for pilocytic or pilomyxoid astrocytomas.

ABBREVIATIONS: rCBV = relative cerebral blood volume; TSITC = tissue signal-intensity time curves; WHO = World Health Organization

Primary brain tumors represent 29% of all childhood cancers, are the most common solid childhood tumor, and are the leading cause of cancer death in this age population.[1] With experienced pediatric neuroimaging specialists, presurgical diagnosis with anatomic MR imaging sequences can be accurate, especially with a classic appearance and location. However, many primary neoplasms do not follow the classic imaging appearance, and advanced imaging techniques such as perfusion imaging, diffusion-weighted imaging, and MR spectroscopy have been used to grade primary pediatric tumors.[2-4]

Dynamic susceptibility contrast perfusion MR imaging has demonstrated utility in the pretreatment evaluation of adult intracranial neoplasms for tumor grading, guiding biopsy, and prognosis. However, while the most common adult primary parenchymal neoplasms are of the astrocytic cell type, the most common pediatric primary brain tumors have diverse cellular origins, with astrocytic origin for pilocytic astrocytomas and embryonal neuroepithelial origin for medulloblastomas. Even within astrocytomas, outside of the classic "cyst and mural nodule" appearance of pilocytic astrocytomas, there is some overlap in the radiographic and histologic appearance of pilocytic astrocytomas and high-grade gliomas, with relative cerebral volume (rCBV) demonstrating usefulness in distinguish-

Received May 6, 2015; accepted after revision July 20.

From the Department of Radiology, Indiana University School of Medicine, Indianapolis, Indiana.

Paper previously presented in part at: American Society of Neuroradiology Annual Meeting and the Foundation of the ASNR Symposium, May 17–22, 2014; Montreal, Quebec, Canada.

Please address correspondence to Chang Ho, MD, 705 Riley Hospital Dr, MRI Department, Indianapolis, IN 46202; e-mail: cyho@iupui.edu

http://dx.doi.org/10.3174/ajnr.A4559

ing the 2 astrocytic entities.[5] However, when the most common pediatric primary brain tumors are evaluated, there is an overlapping range of rCBV values, particularly between pilocytic astrocytomas and medulloblastomas, limiting the usefulness of DSC perfusion in predicting low- versus high-grade tumors preoperatively.[2]

While rCBV has received the greatest attention in differentiating tumor grades from perfusion imaging in adult tumors,[6-8] tissue signal-intensity time curves (TSITC) have also demonstrated diagnostic utility, most notably in differentiating primary CNS lymphoma from glioblastoma multiforme and metastases.[9-11] We evaluated the interobserver agreement of the classification of DSC perfusion MR imaging TSITC and the utility of curve classification as a tool for grading pediatric brain tumors.

MATERIALS AND METHODS

Following institutional review board approval, a retrospective radiology data base search from September 2009 to August 2013 identified 65 patients with pediatric brain tumors with pathology-proved diagnosis and assigned World Health Organization (WHO) grade who had undergone DSC perfusion MR imaging on the initial evaluation before chemotherapy, biopsy, or surgical resection. In most cases, a single dose of 2 mg/kg of IV dexamethasone was given emergently before MR imaging for the treatment of tumor-associated cerebral edema. Two cases were excluded leaving 63 cases for review. One case was excluded due to poor contrast bolus, and the second case, due to susceptibility artifacts generated by the patient's dental braces. This study population was previously reported.[2]

MR Imaging

DSC perfusion MR images were obtained during the first pass of a bolus of gadobenate dimeglumine (MultiHance; Bracco Diagnostics, Princeton, New Jersey) on 1.5T and 3T MR imaging scanners (Magnetom, Avanto and Verio; Siemens, Erlangen, Germany) by using a gradient-echo echo-planar sequence (TR, 1410–2250 ms/TE, 30 and 45 ms; flip angle, 90°). Two different TEs were used on different scanners. A range of TRs was adjusted for tumor coverage. No scans were obtained with a preload of IV contrast. Following a precontrast phase to establish a baseline, a contrast medium dose of 0.1 mmol/kg of body weight was injected followed by a normal saline flush for a total volume of 32 mL. When possible, an 18- or 20-ga peripheral intravenous access was used with a power injector rate of 5 mL/s. In some cases, primarily with smaller children, only 24-ga peripheral intravenous access was possible. Contrast bolus adequacy was evaluated by 2 fellowship-trained board-certified neuroradiologists with a Certificate of Added Qualification (C.Y.H., 7 years' experience, and S.F.K., 3 years' experience) on the basis of TSITC and the patient scan was included or excluded in consensus.

Data Analysis

Using a commercially available workstation (DynaSuite Neuro 3.0; InVivo, Gainesville, Florida), each neuroradiologist independently selected multiple 3- to 5-mm^2 ROIs within the tumor, placed at the locations of perceived highest rCBV by using DynaSuite-generated rCBV maps, blinded to the pathologic diagnosis. Anatomic MR imaging sequences were used to help define tumor location and avoid major blood vessels or hemorrhage when placing the ROI. The resulting signal-intensity curve from the ROI with the highest rCBV was used for classification. This technique has been previously described in the literature.[2] Use of the maximum rCBV for characterization of the TSITC ensures that the most perfused portion of a heterogeneous tumor is evaluated, reducing sampling errors. Curves were assessed out to 50 TRs on the time axis. A y-axis value before the first-pass bolus was chosen to represent the average of the baseline and was compared with the final y-axis value at 50 TRs. The portion of the curve following the first pass of contrast medium bolus was characterized as returning to a level within ±10% of the baseline with a plateau (return to baseline; Fig 1), overshooting at least 10% above the baseline without a plateau (T1-dominant contrast leakage; Fig 2), or failing to return to a level <10% below baseline (T2*-dominant contrast leakage; Fig 3). Interobserver agreement was assessed by using the Cohen κ. Blinded consensus opinion was obtained in cases with discrepant curve classification, and the resulting TSITC were compared with individual WHO tumor grades. TSITC results were also compared with the averaged rCBV maximum between the 2 observers. Histopathologic evaluation of surgical specimens for all tumors was performed by 1 of 2 board-certified neuropathologists who determined a diagnosis and assigned a WHO grade of I through IV.

A χ^2 test of independence was used to assess potential significant differences between 1.5T and 3T, 30- and 45-ms TE, the range of TRs, and dexamethasone administration. Diagnostic accuracy was assessed for specific curve patterns.

Statistical analysis was performed by using SPSS 21 (IBM, Armonk, New York) and an on-line statistical calculator (VassarStats, http://vassarstats.net/).

RESULTS

Patient characteristics are summarized in Table 1. There were 38 low-grade (WHO grade I–II) tumors and 25 high-grade (WHO grade III–IV) tumors.

Independent classification of TSITC by 2 neuroradiologists had a Cohen κ of 0.69 (95% CI, 0.54–0.84), indicating good interobserver agreement. The proportion of agreement was highest with a T1-dominant pattern ($K = 0.79$, 95% CI, 0.56–0.91) compared with T2*-dominant pattern ($K = 0.60$, 95% CI, 0.39–0.78) and return to baseline ($K = 0.57$, 95% CI, 0.35–0.76).

The χ^2 test for independence between 1.5T and 3T scanners ($P = .63$), 30- and 45-ms TE ($P = .55$), and TR range ($P = .14$) failed to show significance, indicating that the null hypothesis is not rejected or that leakage patterns are not dependent on the differences in magnet strength, TE, or TR in our scanning parameters. Dexamethasone, however, did show some significant ($P = .02$) effects. Further χ^2 analysis between tumors treated with dexamethasone ($n = 41$) and without dexamethasone ($n = 22$) showed a significant difference in all low-grade tumors ($P = .03$) but not with pilocytic astrocytomas ($P = .99$), pilomyxoid astrocytomas ($P = 1.0$), or both piloid tumors together ($P = .46$). For high-grade tumors, dexamethasone also did not show a significant effect ($P = .09$).

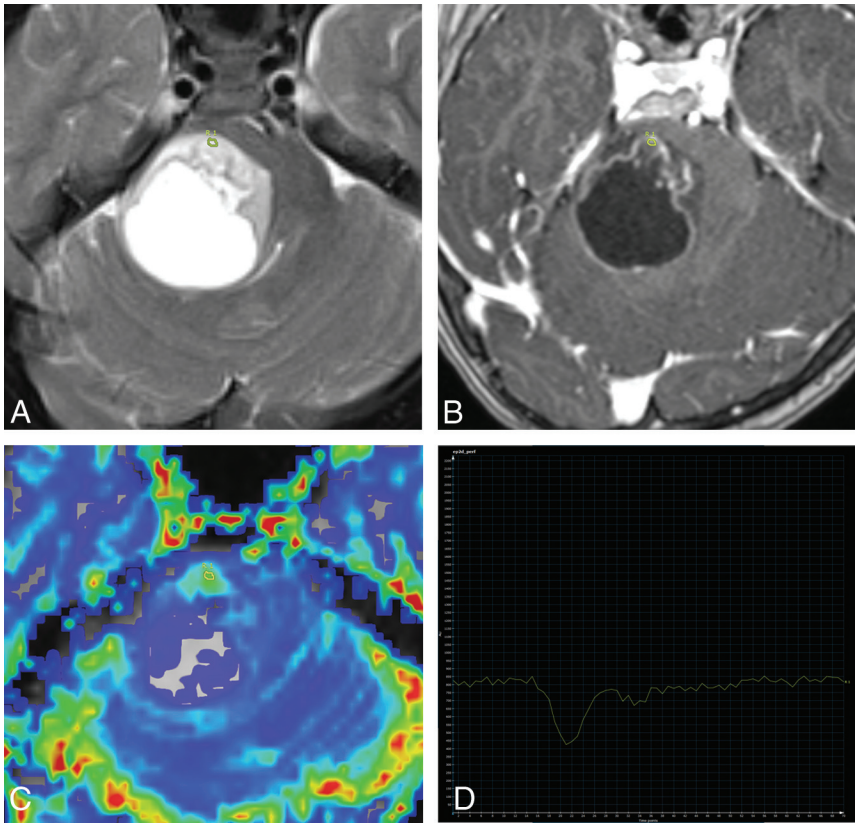

FIG 1. Axial T2 (*A*), axial T1-weighted postcontrast (*B*), axial DSC perfusion CBV map (*C*), and tissue signal-intensity time curve (*D*) of a glioblastoma. The tumor has T2 hyperintensity, cystic change, and minimal heterogeneous enhancement and has well-circumscribed margins suggesting a low-grade neoplasm such as a pilocytic astrocytoma. However, the TSITC from an ROI with the highest tumoral rCBV demonstrates a return to baseline pattern, which is highly sensitive for a high-grade tumor; there is low probability that this represents a pilocytic or pilomyxoid astrocytoma.

astrocytoma, demonstrated predominantly T1-dominant leakage: 15/17 for pilocytic astrocytoma and 6/6 for pilomyxoid astrocytoma. One case of 3 WHO II ependymomas showed T1-dominant leakage. For the diagnosis of pilocytic or pilomyxoid astrocytoma, a T1-dominant leakage pattern yields a high sensitivity (0.91, 95% CI, 0.70–0.98; negative predictive value, 0.95; 95% CI, 0.81–0.99) and specificity (0.90, 95% CI, 0.75–0.97; positive predictive value, 0.84; 95% CI, 0.63–0.95) (Table 2).

An analysis of variance showed no significant differences ($P = .11$, F ratio $= 2.32$) between the means of the rCBV maximum for each leakage pattern (T1-dominant $= 3.25 \pm 3.3$, baseline $= 3.25 \pm 2.2$, T2*-dominant $= 5.18 \pm 3.6$). A t test between the means of rCBV maximum for T1-dominant leakage (3.25 ± 3.3) and T2*-dominant combined with baseline leakage patterns (4.02 ± 2.93) also yielded no significant difference ($P = .33$). χ^2 tests were performed for significant differences between WHO grade and TSITC leakage results. Grade I-versus-II tumors were not significant ($P = .38$) nor were grade III-versus-IV tumors ($P = .93$). Only high (III and IV) versus low grade (I and II) were significant ($P < .0001$).

All Tumors

Among 38 low-grade tumors, 25 had a consensus classification of T1-dominant contrast leakage, while 13 had a consensus curve classification other than T1-dominant leakage—either return to baseline or T2*-dominant leakage. The 25 tumors with T1-dominant contrast leakage included the following: 15 pilocytic astrocytomas, 6 pilomyxoid astrocytomas, 1 low-grade glioneuronal tumor, 1 WHO grade II ependymoma, 1 desmoplastic infantile ganglioglioma, and 1 choroid plexus papilloma. Tumors showing a consensus curve classification with T2*-dominant leakage or return to baseline were predominantly high-grade. Ten of 15 tumors identified as having a postbolus curve with T2*-dominant leakage were high-grade (positive predictive value, 0.67; 95% CI, 0.39–0.87), and 15 of 23 tumors with curves identified as returning to baseline were high-grade (positive predictive value, 0.65; 95% CI, 0.43–0.83). Combining T2* and return-to-baseline patterns for high-grade tumor yielded a high sensitivity (1.0, 95% CI, 0.83–1.0) and negative predictive value (1.0; 95% CI, 0.83–1.0) at the cost of specificity (0.66, 95% CI, 0.49–0.80). The most common high-grade tumors such as medulloblastoma, anaplastic ependymoma, and glioblastoma had both T2* and baseline patterns. All 3 cases of atypical teratoid/rhabdoid tumor showed a return to baseline pattern. Conversely, the most common low-grade tumors, such as pilocytic astrocytoma and pilomyxoid

Dexamethasone Group

Among the 41 patients with tumors who received dexamethasone before DSC perfusion MR imaging, 19 had a consensus T1-dominant leakage, 12 had a consensus T2*-dominant leakage pattern, and 10 had a consensus return to baseline pattern. All 19 with a T1-dominant leakage pattern were low-grade tumors while 5 other low-grade tumors had a leakage pattern other than T1-dominant leakage. Of 12 tumors with T2*-dominant leakage, 9 were high-grade. Of 10 tumors with a return-to-baseline pattern, 8 were high-grade. Thirteen of 14 pilocytic astrocytomas and 3 of 3 pilomyxoid astrocytomas demonstrated T1-dominant leakage. Diagnostic accuracy for this cohort is summarized in Table 2. Within the entire dexamethasone group, no significant differences were seen between magnet strengths ($P = .62$), TE ($P = .32$), or TR ($P = .20$).

No Dexamethasone Group

Among the 22 patients with tumors who did not receive dexamethasone before DSC perfusion MR imaging, 6 had a consensus T1-dominant leakage, 3 had a consensus T2*-dominant leakage, and 13 had a consensus return to baseline pattern. All 6 tumors with a T1-dominant leakage pattern were low-grade tumors. Eight low-grade tumors had a leakage pattern other

than T1-dominant leakage. Of the 3 tumors with T2*-dominant leakage, only 1 was high-grade. Of 13 tumors with return-to-baseline patterns, 7 were high-grade. Two of 3 pilocytic astrocytomas and 3 of 3 pilomyxoid astrocytomas demonstrated T1-dominant leakage. Diagnostic accuracy is summarized in Table 2. Within the entire no dexamethasone group, no significant differences were seen among magnet strength ($P = .08$), TE ($P = .97$), or TR ($P = .40$).

DISCUSSION

In practice, hemodynamics, status of the blood-brain barrier, timing of the contrast bolus, and MR pulse sequence parameters affect the shape of the TSITC.[12-16] Disruption or lack of a blood-brain barrier results in leakage of contrast medium into the extravascular extracellular space. While in the intravascular space, paramagnetic contrast medium causes predominantly T2* effects with loss of MR signal; however, once in the extravascular extracellular space, T1-shortening effects compete with the T2* effects.[15,16] Depending on the MR imaging parameters and biologic tissue environment, T1-shortening effects may predominate and cause a postbolus curve that returns to and then passes baseline, or T2* effects may predominate and result in a postbolus curve that fails to return to baseline.[15] Another mechanism for a curve that fails to return to baseline was suggested by Kassner et al,[13] who showed that residual T2* effects may reflect delayed passage of intravascular contrast medium due to vascular tortuosity, disorganization, and hypoperfusion in areas of increased neovascularity. They compared this effect with the tumor staining seen on conventional angiography.

Previous authors described the portion of the curve after the peak as "percent signal recovery,"[9,17] with a high percent signal recovery correlating with our T1-dominant leakage; a low percent signal recovery, T2*-dominant leakage; or with smaller T2* effects, a return to baseline. Cha et al[17] demonstrated a significant difference between metastatic brain tumors and glioblastoma and the associated surrounding abnormal white matter in adults, with greater T2* effects and <50% return to baseline for metastatic tumors compared with >75% re-

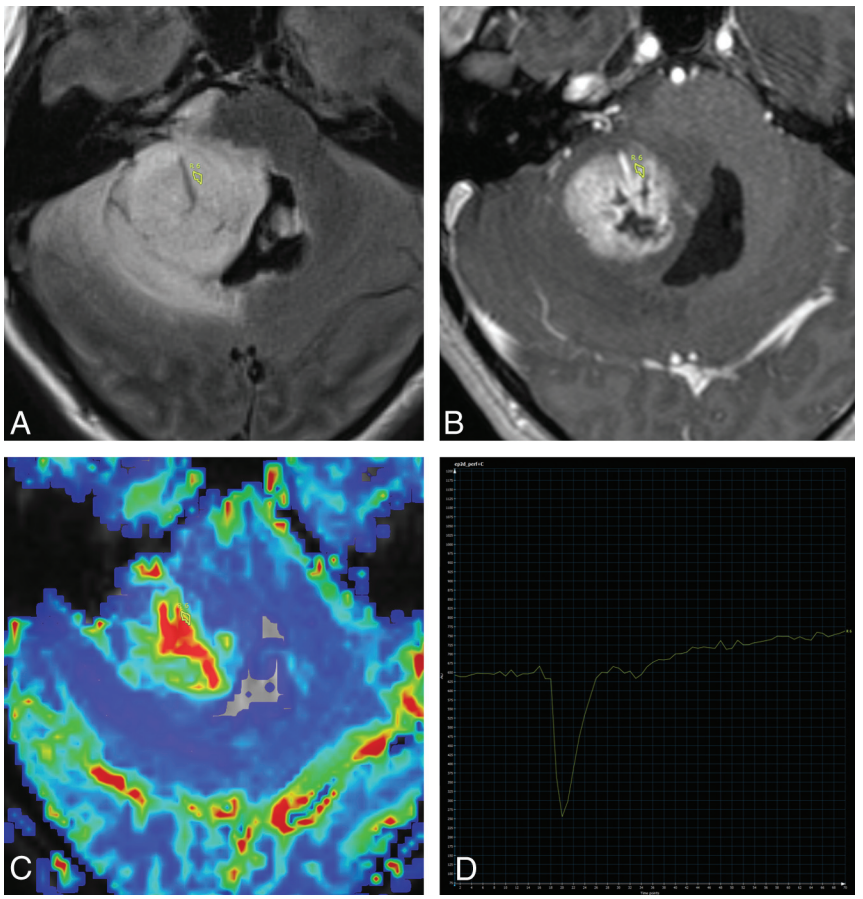

FIG 2. Axial T2 FLAIR (*A*), axial T1-weighted postcontrast (*B*), axial DSC perfusion rCBV map (*C*), and tissue signal-intensity time curve (*D*) of a pilocytic astrocytoma with atypical appearance. Despite apparent increased rCBV, poorly defined margins, central necrosis, and surrounding T2 hyperintensity suggesting a high-grade neoplasm, the T1-dominant leakage pattern suggests the correct interpretation of a low-grade tumor. The ROI is placed in the highest perfusing portion of the tumor, not including a dominant central vessel.

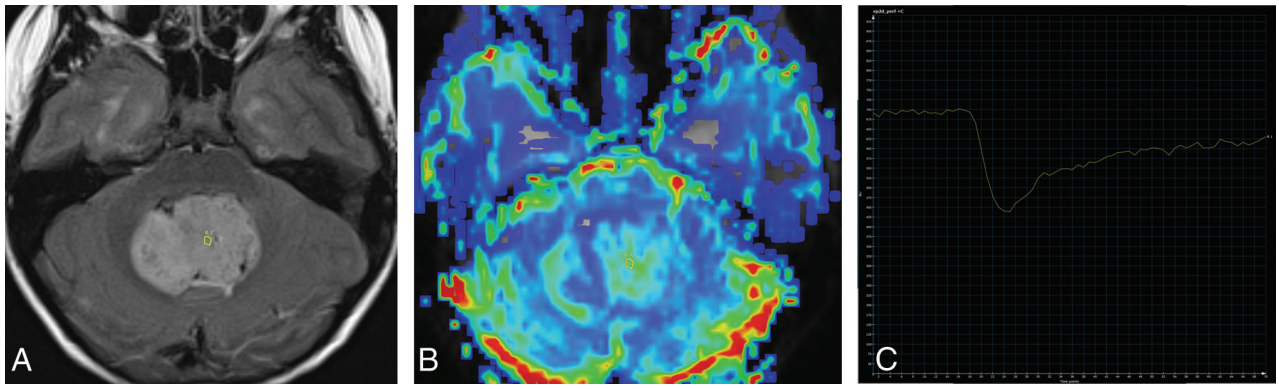

FIG 3. Axial T2 FLAIR (*A*), axial DSC perfusion rCBV map (*B*), and tissue signal-intensity time curve (*C*) in a patient with medulloblastoma. The tissue signal-intensity time curve demonstrates T2*-dominant contrast leakage following the contrast bolus.

covery for glioblastomas. They suggested that this difference is due to the lack of a blood-brain barrier, leading to greater uniform vascular permeability and leakage in metastatic tumors compared with some presence of a blood-brain barrier in glioblastomas, with less uniform vascular permeability.[17] Last, the balance between T1 and T2* effects is affected by varying MR imaging parameters, including the flip angle, TE, and TR in gradient-echo EPI DSC perfusion MR imaging.[10,12,13,15-17] We used a narrow range of TEs for similar T2* effects across scanners and a uniform flip angle on all scanners for recovery from the peak. Previous authors have used a low flip angle to suppress T1 signal effects[16,17]; however in our study, our 90° flip angle did not sufficiently suppress the T1 signal for our range of TRs to prevent overshooting the baseline in most low-grade tumors, which we categorized as T1-dominant leakage.

Advances in Knowledge

A striking finding in our data was 100% positive predictive value (25 of 25) for low-grade tumors if a T1-dominant leakage pattern was identified. The converse is also true in that the lack of a T1 leakage pattern (T2* or return to baseline) resulted in a 100% negative predictive value for high-grade tumors. T1-dominant leakage patterns were also sensitive and specific for either a pilocytic astrocytoma or pilomyxoid astrocytoma. In addition, good interobserver agreement for identifying a T1-dominant leakage pattern was found, indicating potential clinical utility for grading pediatric brain tumors with TSITC from DSC perfusion.

Little prior data exist in the literature regarding the use of DSC perfusion MR imaging and signal-intensity curves in the evaluation of pediatric brain tumors. Similar to our findings, Grand et al[18] reported a series of 9 pilocytic astrocytomas evaluated with DSC perfusion MR imaging, in which all 9 tumors demonstrated an overshooting of the baseline or a T1-dominant contrast leakage pattern. Cha et al reported that pilocytic astrocytomas have >70% signal recovery, while medulloblastomas have <50% signal recovery, which is consistent with our findings.[19]

Before our study, a T1-dominant leakage pattern has most notably been demonstrated in primary CNS lymphoma and has been shown to be useful in distinguishing lymphoma from glioblastoma multiforme and CNS metastases.[9-11] Despite the lack of neoangiogenesis in CNS lymphoma, both glioblastoma and lymphoma have elevated rCBV but a significant difference in the high percent signal recovery for lymphomas. These features have been

Table 1: Tumor pathology with patient age and TSITC results

		Age (yr)		Tissue Signal-Intensity Time Curve Classification		
	Cases	Average	Range	T1	Baseline	T2
All cases	63	6.3	1.0–16.8	25	23	15
Infratentorial	39	5.6	1.2–14.2	16	13	10
Supratentorial	24	7.4	1.0–16.8	9	10	5
WHO I	25	7.1	1.1–15.0	18	5	2
WHO II	13	5.9	1.2–16.8	7	3	3
WHO III	9	4.6	1.4–12.0	0	6	3
WHO IV	16	6.4	1.0–16.2	0	9	7
Pilocytic astrocytoma	17	7.3	2.2–15.0	15	1	1
Medulloblastoma	9	6.8	2.3–13.3	0	4	5
Ependymoma WHO III	7	4.3	1.4–12.0	0	4	3
Pilomyxoid astrocytoma	6	2.9	1.2–5.8	6	0	0
Ependymoma WHO II	3	2.2	1.5–2.9	1	0	2
ATRT	3	1.4	1.0–1.9	0	3	0
GBM	3	6.9	4.2–9.5	0	2	1
Choroid plexus papilloma	2	4.1	3.1–5.2	1	1	0
Fibrillary astrocytoma	1	4.3		0	1	0
Craniopharyngioma	1	5.5		0	1	0
Desmoplastic infantile ganglioglioma	1	1.1		1	0	0
Ganglioglioma	1	12.9		0	1	0
Ganglion cell tumor	1	1.8		0	1	0
High-grade diffuse glioma	1	6.9		0	1	0
Low-grade glioma	1	12.8		0	0	1
Low-grade glioneuronal tumor	1	11.5		1	0	0
Low-grade oligoastrocytoma	1	16.8		0	1	0
Oligodendroglioma	1	15.5		0	1	0
Pineal parenchymal tumor WHO II	1	15.6		0	0	1
Supratentorial PNET	1	16.2		0	0	1
Anaplastic astrocytoma	1	4		0	1	0

Note:—ATRT indicates atypical teratoid rhabdoid tumor; GBM, glioblastoma multiforme; PNET, primitive neuroectodermal tumor.

Table 2: Diagnostic sensitivity of leakage patterns and tumors with 95% confidence intervals

	Sensitivity	Specificity	PPV	NPV
T1 leakage pattern for low-grade tumors	66% (49%–80%)[a]	100% (83%–100%)[ba]	100% (83%–100%)[ba]	66% (49%–80%)[a]
	79% (57%–92%)[b]	100% (77%–100%)[b]	100% (79%–100%)[b]	77% (54%–91%)[b]
	43% (19%–70%)[c]	100% (60%–100%)[c]	100% (52%–100%)[c]	50% (26%–74%)[c]
T2* leakage and baseline patterns for high-grade tumors	100% (83%–100%)[a]	66% (49%–80%)[a]	66% (49%–80%)[a]	100% (83%–100%)[a]
	100% (77%–100%)[b]	79% (57%–92%)[b]	77% (54%–91%)b	100% (79%–100%)[b]
	100% (60%–100%)[c]	43% (19%–70%)[c]	50% (26%–74%)[c]	100% (52%–100%)[c]
T1 leakage for pilocytic and pilomyxoid astrocytomas	91% (70%–98%)[a]	90% (75%–97%)[a]	84% (63%–95%)[a]	95% (81%–99%)[a]
	94% (69%–100%)[b]	88% (67%–97%)[b]	84% (60%–96%)[b]	95% (75%–100%)[b]
	83% (36%–99%)[c]	94% (68%–100%)[c]	83% (36%–99%)[c]	94% (68%–100%)[c]

Note:—PPV indicates positive predictive value; NPV, negative predictive value.

[a] All tumor results.

[b] Dexamethasone tumors results.

[c] Nondexamethasone tumors results.

attributed to the characteristic perivascular invasion of lymphoma cells, leading to disruption of the basement membrane and resulting vascular permeability. The hypercellularity of lymphoma with a small extravascular extracellular space has been suggested as a contributing factor, though the exact mechanism for T1-dominant leakage effects in lymphoma is not well-understood.[9] This finding contradicts the findings of Cha et al[17] in that the lack of a blood-brain barrier in metastatic disease, with resulting vascular permeability, results in a low percent recovery or a T2*-dominant effect rather than the T1-dominant effect in CNS lymphoma.[9,17] Cha et al[17] used a flip angle of 35° compared with 80° for Mangla et al,[9] which may contribute to the differing TSITC results. Biologic factors may include differing rates of contrast leakage between CNS lymphoma and metastatic disease with a faster accumulation and concentration of extravascular contrast in metastatic disease leading to T2*-dominant effects. The mechanism underlying the observed postbolus T1-dominant effects in low-grade pediatric brain tumors is not known but is also likely related to the balance between T1-shortening and T2* effects of paramagnetic contrast medium that has leaked into the extravascular extracellular space. Other factors affecting the T1–T2* balance may include characteristics of the extravascular space such as cellular attenuation, water content, and other molecular constituents, in addition to hemodynamic flow issues and capillary permeability.

Pilocytic astrocytomas and pilomyxoid astrocytomas account for 21 of the 25 tumors in our series demonstrating postbolus T1-dominant leakage. Pilocytic astrocytomas are described as having a biphasic histology with areas of loose glial tissue interposed with compacted piloid tissue composed of attenuated hypercellular sheets of elongated bipolar cells.[20] Distinguishing features of pilomyxoid astrocytomas include monomorphous piloid cells in a myxoid background with an angiocentric pattern, similar to perivascular pseudorosettes in ependymomas. While pilomyxoid astrocytomas tend to occur in younger children in the hypothalamic/chiasmatic pathway, with more aggressive behavior and a higher propensity for leptomeningeal spread, pilocytic and pilomyxoid astrocytomas have large morphologic and imaging overlap. There have been reports of recurrent pilomyxoid tumors demonstrating pilocytic features after several years, with some authors suggesting that pilomyxoid astrocytoma may be an infantile form versus an extreme subtype of pilocytic astrocytoma.[21-23] Because of this overlap and the lack of distinguishing imaging characteristics between the 2 tumors, we calculated diagnostic accuracy with both tumors rather than separately. Vascular proliferation can be seen in the solid component of both tumors but with more mature endothelial cells in a single layer compared with glioblastomas.[24,25] These single endothelial layers with open tight junctions and fenestrae and hyaline degeneration around vessels have been postulated to allow contrast medium extravasation and therefore vascular permeability.[18] Similar to CNS lymphomas, this level of increased vascular permeability likely plays a partial but crucial role in the T1-dominant leakage effects seen in both tumors. Further research between different pediatric tumors by using T1 signal–based dynamic contrast-enhanced MR imaging may be helpful in elucidating differences in vascular permeability.

Effect of Dexamethasone on Leakage Patterns

We could not control for the administration of dexamethasone in pediatric patients with newly diagnosed brain tumors because corticosteroids are a first-line emergent therapy for controlling the cerebral swelling and the resultant mass effect from mass-occupying brain tumors. In a previous work on the same patient population, there was no significance between patients with and without dexamethasone treatment and rCBV measurements.[2] However, given the known rapid effects of dexamethasone in decreasing capillary permeability and reducing vasogenic edema,[26,27] the significance between patient populations is not surprising. However, only our low-grade tumor group was significant, and there was a larger proportion of T1-dominant and T2*-dominant leakage patterns within the dexamethasone group. This result seems counterintuitive because high-grade tumors typically have greater vasogenic edema and mass effect, and decreasing capillary permeability should trend toward the return to baseline pattern because this pattern would best represent no leakage. In reality, multiple physiologic parameters likely affect the leakage pattern as indicated by our results. Despite the significance of dexamethasone on the low-grade tumor group, the 100% specificity of a T1-dominant leakage pattern for low-grade pediatric tumors and the high sensitivity and specificity for piloid astrocytomas remain unchanged for both groups with or without dexamethasone.

Implications for Patient Care

Despite uncertainty in the exact underlying mechanism, a T1-dominant contrast leakage pattern on the signal-intensity curve obtained in the region of highest tumor rCBV is empirically highly predictive for low-grade brain tumor in the pediatric population, while a T2*-dominant or baseline pattern has high sensitivity for a high-grade tumor. In addition to rCBV data,[2] TSITC from DSC perfusion potentially offer additional information not otherwise apparent with routine anatomic MR imaging sequences. Recognition of a T1-dominant leakage pattern may improve accuracy in preoperatively predicting the presence of a low-grade pediatric brain tumor. While experienced pediatric neuroradiologists can recognize low-versus-high-grade tumors in most cases, recognition of this pattern of perfusion leakage may be very helpful in the minority of cases in which low-grade pilocytic or pilomyxoid astrocytomas become large and heterogeneous, mimicking higher grade neoplasms and, conversely, when high-grade astrocytomas have benign imaging features (Figs 1 and 2). Furthermore, when complete surgical resection is not possible, knowing the likelihood of a high-grade or low-grade tumor can guide how aggressive a neurosurgeon should be in debulking the tumor, at the risk of morbidity and mortality.

Limitations

The neuroradiologists evaluating the perfusion data were not blinded to the anatomic MR imaging sequences, some of which were highly suggestive of the tumor diagnosis. This scenario was unavoidable because the anatomic images provide information integral to the assessment of the perfusion images (eg, location of tumor, location of major vessels, and so forth). This limitation is reasonable however because it reflects the process in which MR

perfusion images are evaluated in clinical practice. As noted in the discussion, a T1-dominant contrast leakage pattern has been described in CNS lymphoma, and our series of 63 pediatric brain tumors included no cases of CNS lymphoma. While this represents a potential pitfall in using a T1-dominant leakage pattern to classify pediatric brain tumors as low grade, CNS lymphoma is rarely encountered in the pediatric population. Contrast medium infusion rate and peripheral intravenous catheter gauge are related issues that likely affect the quality of the perfusion study and are recognized challenges in performing DSC perfusion MR imaging on pediatric patients.[28] However, only 1 study of the 65 identified by the search criteria was excluded for poor contrast medium bolus, indicating that high-quality DSC perfusion MR imaging can be performed in pediatric patients with brain tumors. Differences in TR and TE parameters corresponded to those in studies obtained on different 1.5T and 3T scanners and theoretically have some effect on signal intensity and recovery/leakage patterns. However, our analysis demonstrates no significant differences in our results attributable to these different field strengths or parameters. There are no standardized criteria in the literature for T1 leak/T2* leak or return to baseline. We arbitrarily chose the ±10% range for the curve classification as a means of separation; consequently, curve classification could be altered if different thresholds are used. Similarly, as previously described, larger differences in technical parameters (flip angle, TE, TR) may result in greater differences in curve classification.

CONCLUSIONS

There is good interobserver agreement in the classification of the DSC perfusion tissue signal-intensity time curves for pediatric brain tumors. Among our population of pediatric patients with brain tumors, a T1-dominant leakage pattern is 100% specific for a low-grade tumor and sensitive and specific for piloid astrocytomas, regardless of dexamethasone treatment. The addition of tissue signal-intensity time curves may help in cases in which low-grade tumors are large and heterogeneous, mimicking high-grade neoplasms.

Disclosures: Chen Lin—*UNRELATED*: *Consultancy*: CIVCO Medical Solutions*; *Grants/Grants Pending*: Siemens.* *Money paid to the institution.

REFERENCES

1. Ostrom QT, de Blank PM, Kruchko C, et al. **Alex's Lemonade Stand Foundation Infant and Childhood Primary Brain and Central Nervous System Tumors Diagnosed in the United States in 2007–2011.** *Neuro Oncol* 2015;1(suppl 10):x1–x36 CrossRef Medline
2. Ho CY, Cardinal JS, Kamer AP, et al. **Relative cerebral blood volume from dynamic susceptibility contrast perfusion in the grading of pediatric primary brain tumors.** *Neuroradiology* 2015;57:299–306 CrossRef Medline
3. Kralik SF, Taha A, Kamer AP, et al. **Diffusion imaging for tumor grading of supratentorial brain tumors in the first year of life.** *AJNR Am J Neuroradiol* 2014;35:815–23 CrossRef Medline
4. Panigrahy A, Nelson MD Jr, Blüml S. **Magnetic resonance spectroscopy in pediatric neuroradiology: clinical and research applications.** *Pediatr Radiol* 2010;40:3–30 CrossRef Medline
5. de Fatima Vasco Aragao M, Law M, Batista de Almeida D, et al. **Comparison of perfusion, diffusion, and MR spectroscopy between low-grade enhancing pilocytic astrocytomas and high-grade astrocytomas.** *AJNR Am J Neuroradiol* 2014;35:1495–502 CrossRef Medline
6. Law M, Yang S, Wang H, et al. **Glioma grading: sensitivity, specificity, and predictive values of perfusion MR imaging and proton MR spectroscopic imaging compared with conventional MR imaging.** *AJNR Am J Neuroradiol* 2003;24:1989–98 Medline
7. Law M, Young R, Babb J, et al. **Histogram analysis versus region of interest analysis of dynamic susceptibility contrast perfusion MR imaging data in the grading of cerebral gliomas.** *AJNR Am J Neuroradiol* 2007;28:761–66 Medline
8. Morita N, Wang S, Chawla S, et al. **Dynamic susceptibility contrast perfusion weighted imaging in grading of nonenhancing astrocytomas.** *J Magn Reson Imaging* 2010;32:803–08 CrossRef Medline
9. Mangla R, Kolar B, Zhu T, et al. **Percentage signal recovery derived from MR dynamic susceptibility contrast imaging is useful to differentiate common enhancing malignant lesions of the brain.** *AJNR Am J Neuroradiol* 2011;32:1004–10 CrossRef Medline
10. Hartmann M, Heiland S, Harting I, et al. **Distinguishing of primary cerebral lymphoma from high-grade glioma with perfusion-weighted magnetic resonance imaging.** *Neurosci Lett* 2003;338:119–22 CrossRef Medline
11. Sugahara T, Korogi Y, Shigematsu Y, et al. **Perfusion-sensitive MRI of cerebral lymphomas: a preliminary report.** *J Comput Assist Tomogr* 1999;23:232–37 CrossRef Medline
12. Hu LS, Baxter LC, Pinnaduwage DS, et al. **Optimized preload leakage-correction methods to improve the diagnostic accuracy of dynamic susceptibility-weighted contrast-enhanced perfusion MR imaging in posttreatment gliomas.** *AJNR Am J Neuroradiol* 2010;31:40–48 CrossRef Medline
13. Kassner A, Annesley DJ, Zhu XP, et al. **Abnormalities of the contrast re-circulation phase in cerebral tumors demonstrated using dynamic susceptibility contrast-enhanced imaging: a possible marker of vascular tortuosity.** *J Magn Reson Imaging* 2000;11:103–13 Medline
14. Jackson A, Kassner A, Annesley-Williams D, et al. **Abnormalities in the recirculation phase of contrast agent bolus passage in cerebral gliomas: comparison with relative blood volume and tumor grade.** *AJNR Am J Neuroradiol* 2002;23:7–14 Medline
15. Paulson ES, Schmainda KM. **Comparison of dynamic susceptibility-weighted contrast-enhanced MR methods: recommendations for measuring relative cerebral blood volume in brain tumors.** *Radiology* 2008;249:601–13 CrossRef Medline
16. Boxerman JL, Paulson ES, Prah MA, et al. **The effect of pulse sequence parameters and contrast agent dose on percentage signal recovery in DSC-MRI: implications for clinical applications.** *AJNR Am J Neuroradiol* 2013;34:1364–69 CrossRef Medline
17. Cha S, Lupo JM, Chen MH, et al. **Differentiation of glioblastoma multiforme and single brain metastasis by peak height and percentage of signal intensity recovery derived from dynamic susceptibility-weighted contrast-enhanced perfusion MR imaging.** *AJNR Am J Neuroradiol* 2007;28:1078–84 CrossRef Medline
18. Grand SD, Kremer S, Tropres IM, et al. **Perfusion-sensitive MRI of pilocytic astrocytomas: initial results.** *Neuroradiology* 2007;49:545–50 CrossRef Medline
19. Cha S. **Dynamic susceptibility-weighted contrast-enhanced perfusion MR imaging in pediatric patients.** *Neuroimaging Clin N Am* 2006;16:137–47, ix CrossRef Medline
20. Koeller KK, Rushing EJ. **From the archives of the AFIP: pilocytic astrocytoma: radiologic-pathologic correlation.** *Radiographics* 2004;24:1693–708 CrossRef Medline
21. Chikai K, Ohnishi A, Kato T, et al. **Clinico-pathological features of pilomyxoid astrocytoma of the optic pathway.** *Acta Neuropathol* 2004;108:109–14 Medline
22. Ceppa EP, Bouffet E, Griebel R, et al. **The pilomyxoid astrocytoma and its relationship to pilocytic astrocytoma: report of a case and a critical review of the entity.** *J Neurooncol* 2007;81:191–96 Medline
23. Jeon YK, Cheon JE, Kim SK, et al. **Clinicopathological features and global genomic copy number alterations of pilomyxoid astrocytoma in the hypothalamus/optic pathway: comparative analysis with pilocytic astrocytoma using array-based comparative genomic hybridization.** *Mod Pathol* 2008;21:1345–56 CrossRef Medline

24. Brat DJ, Scheithauer BW, Fuller GN, et al. **Newly codified glial neoplasms of the 2007 WHO Classification of Tumours of the Central Nervous System: angiocentric glioma, pilomyxoid astrocytoma and pituicytoma.** *Brain Pathol* 2007;17:319–24 CrossRef Medline
25. Johnson MW, Eberhart CG, Perry A, et al. **Spectrum of pilomyxoid astrocytomas: intermediate pilomyxoid tumors.** *Am J Surg Pathol* 2010;34:1783–91 CrossRef Medline
26. Jarden JO, Dhawan V, Moeller JR, et al. **The time course of steroid action on blood-to-brain and blood-to-tumor transport of 82Rb: a positron emission tomographic study.** *Ann Neurol* 1989;25:239–45 CrossRef Medline
27. Sinha S, Bastin ME, Wardlaw JM, et al. **Effects of dexamethasone on peritumoural oedematous brain: a DT-MRI study.** *J Neurol Neurosurg Psychiatry* 2004;75:1632–35 CrossRef Medline
28. Yeom KW, Mitchell LA, Lober RM, et al. **Arterial spin-labeled perfusion of pediatric brain tumors.** *AJNR Am J Neuroradiol* 2014;35:395–401 CrossRef Medline